www.elsevier.nl/locate/jorganchem

Journal of Organometallic Chemistry 610 (2000) 80–87

Journal of Organometallic Chemistry

A comparison between CpCo-stabilized cyclopentadienone complexes and their *O*-alkylated or protonated congeners

Rolf Gleiter [a,*], Rolf Roers [a], Frank Rominger [a], Bernhard Nuber [b], Isabella Hyla-Kryspin [a]

[a] *Organisch-Chemisches Institut der Universität Heidelberg, Im Neuenheimer Feld 270, D-69120 Heidelberg, Germany*
[b] *Anorganisch-Chemisches Institut der Universität Heidelberg, Im Neuenheimer Feld 270, D-69120 Heidelberg, Germany*

Received 25 April 2000

Abstract

The CpCo-stabilized tricyclic cyclopentadienone complexes **4** and **6** as well as the cyclopentadienonophane **8** were treated with an excess of triethyloxonium tetrafluoroborate. This yields, in case of **4** and **6**, to the yellow colored *O*-ethylcobalticinium salts **5** and **7**. In the case of **8** the alkylation yielded the mono- and bis-*O*-ethylcobalticinium salts **9** and **10**, respectively. Protonation of the superphane **8** yields to the diprotonated superphane **11**. X-ray investigations allowed a comparison of **5** and **11** with **4** and **8**. This comparison shows that the CpCo units in **4** and **8** are more tightly bound to the butadiene units of the cyclopentadienone rings than to the CO groups. In the case of **5** and **11** the distances to all five carbons of the alkoxycyclopentadienyl units are approximately equal. This difference in the bonding was substantiated by model calculations on (η^5-cyclopentadienone)(η^5-cyclopentadienyl)cobalt (**2**) and its *O*-protonated form **12** as well as (η^4-butadiene)(η^5-cyclopentadienyl)cobalt (**13**) and the cobalticinium ion (**14**). The results show similarities between **2** and **13** as well as **12** and **14**.

Keywords: Cyclopentadienone complexes; *O*-Ethylcobalticinium salts; DFT calculations

1. Introduction

Like cyclobutadiene, cyclopentadienone [1] dimerizes readily via a Diels–Alder cycloaddition. Its existence as a short-lived monomer has been demonstrated by trapping experiments [2]. This behavior has been rationalized on the basis of Hückel-type calculations which show only a small gap between the highest occupied (HOMO) and lowest unoccupied (LUMO) molecular orbitals [3], similar to the orbital sequence predicted for singlet cyclobutadiene. Some derivatives of the uncomplexed cyclopentadienone are known [1], all of them have in common either bulky substituents such as *tert*-butyl- or adamantyl-groups (e.g. **1**) or at least three phenyl rings. These substituents render cyclopentadienone kinetically stable (Formula 1) by preventing its dimerization. A further possibility of stabilizing the cyclopentadienone ring is its complexation with metal fragments. Stable derivatives are known with CpCo and $Fe(CO)_3$ fragments, for example **2** and **3** [4]. This complexation leads to the occupation of the LUMO of the cyclopentadienone ring resulting in a stable species with 18 valence electrons. The electronic structure of the complexes can be described by the resonance structures **2a** and **2b**. The complexation by

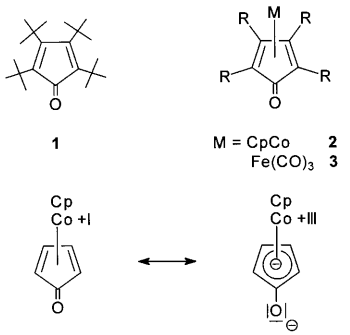

(Formula 1)

* Corresponding author. Tel.: +49-6221-548400; fax: +49-6221-544205.
E-mail address: rolf.gleiter@urz.uni-heidelberg.de (R. Gleiter).

0022-328X/00/$ - see front matter
PII: S0022-328X(00)00431-9

the metal-fragment goes along with a higher electron density at the cyclopentadienone ring as expressed by valence structure **2b** [5]. Consequently, a high-field shift of the ^{13}C signal at the CO group by about 40–50 ppm has been encountered [6]. A further consequence is the higher electron density at the oxygen atoms. This shows up in the protonation [7] and alkylation [6,8] of cyclopentadienone metal complexes. Alkylations have been carried out with dimethylsulfate [8] or trialkyloxonium salts [6].

2. Results

The recent synthesis of polycyclic CpCo complexed cyclopentadienones **4** and **6** as well as the superphane **8** [9] prompted us to carry out alkylation and protonation experiments with these species (Scheme 1). Reaction of **4** and **6** with a threefold excess of triethyloxonium fluoroborate in methylene chloride yielded the yellow colored products **5** and **7**, respectively.

In the ^{1}H-NMR spectrum of **5** and **7** the singlet of the Cp-protons was shifted almost by 1 ppm towards lower field as compared to the starting material. The ^{13}C signal of the ring-carbon atom attached to the ethoxy group was shifted towards lower field by about 25 ppm compared to the CO group.

The reaction of the superphane **8** with an eightfold excess of triethyloxonium fluoroborate yielded two products in the ratio of 4:1 in an overall yield of 50%. The main product was the monoalkylation product **9**, and the side product was the dialkylated product **10** (Scheme 2). The structural assignment of **9** and **10** is based on their NMR spectra. In the case of **9**, two singlets for the Cp protons are found at $\delta = 5.22$ and 4.53. Unfortunately, we could not detect the signal for

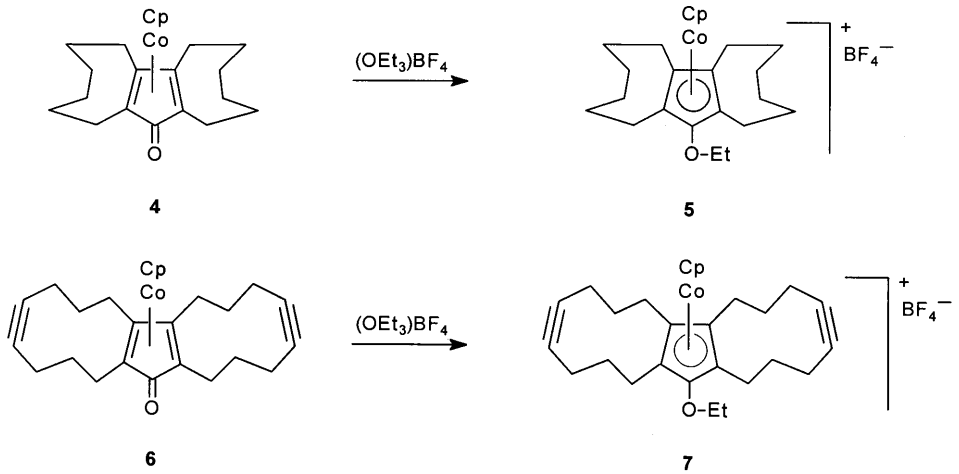

Scheme 1.

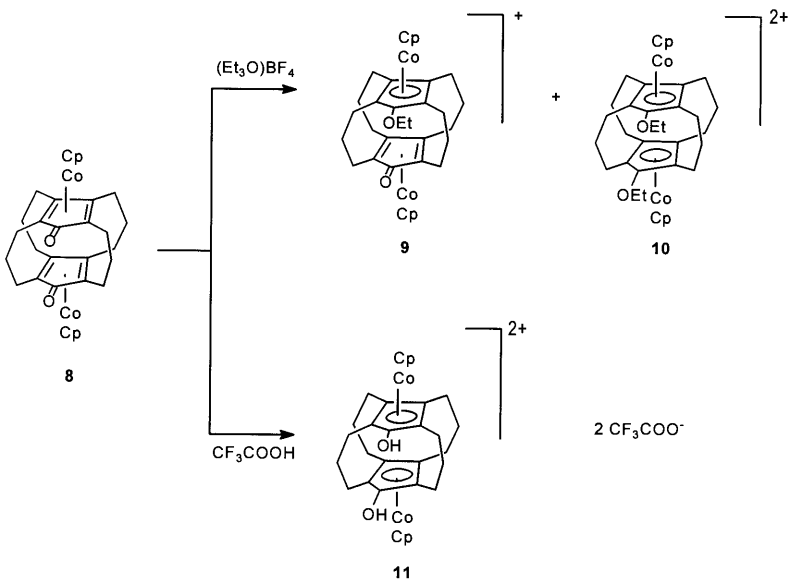

Scheme 2.

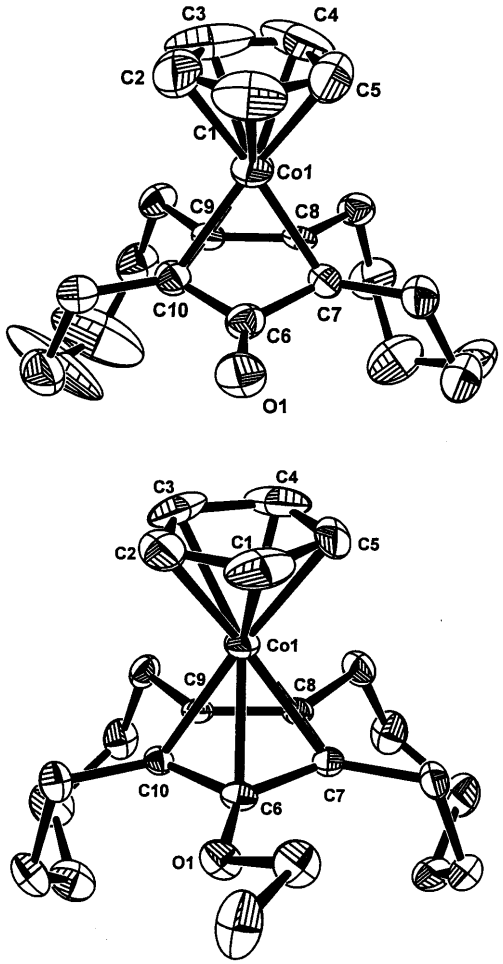

Fig. 1. Comparison between the molecular structures of **4** (top) and **5** (bottom). In the case of **5** the counter ion (Cl^-) is not shown. The hydrogen atoms are omitted for the sake of clarity. The plots are presented at 50% probability of the thermal ellipsoids.

Table 1
Comparison of selected bond lengths (Å) of **4** and **5** [a]

	4	5
Co–C1	2.03(1)	2.035(4)
Co–C2	2.01(1)	2.030(4)
Co–C3	2.03(1)	2.033(4)
Co–C4	2.03(1)	2.040(4)
Co–C5	2.03(1)	2.030(4)
Co–C6	2.26(1)	2.077(3)
Co–C7	2.03(1)	2.042(4)
Co–C8	1.99(1)	2.036(4)
Co–C9	1.98(1)	2.023(4)
Co–C10	2.05(1)	2.049(4)
O1–C6	1.25(1)	1.343(4)

[a] For the numbering see Fig. 1.

CO in the ^{13}C-NMR spectrum of **9**. The ring carbon atom at the ethoxy group was detected at $\delta = 127$. In the case of **10** the corresponding signal appeared at $\delta = 128$. In addition to the twofold alkylation we could also achieve a twofold protonation of **8** to **11** whose NMR results are in line with those of **9** and **10**.

To learn more about the bonding properties of the cyclopentadienone complexes and their protonated and alkylated derivatives, we have carried out X-ray analyses on **5** and **11** and compared the obtained structural parameters with those of the corresponding cyclopentadienone derivatives **4** and **8** [9]. In Fig. 1 the molecular structures of **4** and **5** are presented. In Table 1 we compare the bond distances between cobalt and the

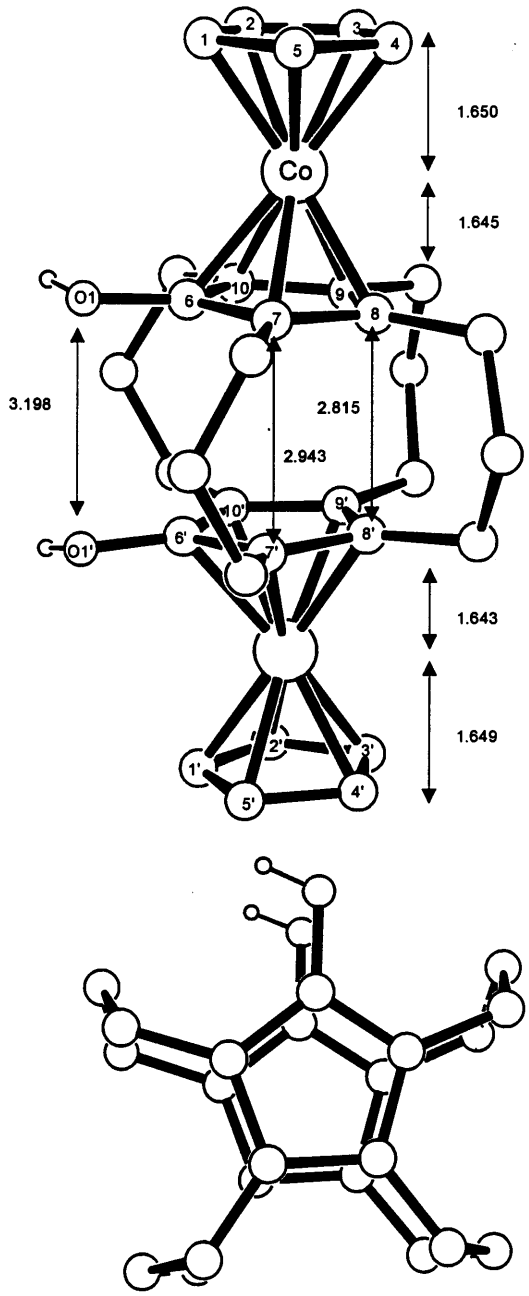

Fig. 2. Side-view of the molecular structure of **11** (top). The counter ion trifluoro acetate is not shown. A top-view of the central frame (bottom) shows the conformation of the bridges. The hydrogen atoms are omitted for the sake of clarity.

Table 2
Comparison of selected bond lengths (Å) of **8** and **11** [a]

	8	**11**
Co–C1	2.038(2)	2.031(3)
Co–C2	2.036(2)	2.035(3)
Co–C3	2.063(2)	2.043(3)
Co–C4	2.068(2)	2.039(3)
Co–C5	2.039(2)	2.029(3)
C6–C6′	3.046(2)	3.045(3)
C7–C7′	3.004(2)	2.943(3)
C8–C8′	2.826(2)	2.815(3)
Co–C6	2.154(2)	2.064(3)
Co–C7	2.076(2)	2.065(3)
Co–C8	2.015(2)	2.031(3)
Co–C9	2.014(2)	2.026(3)
Co–C10	2.075(2)	2.062(3)
C6–O1	1.278(2)	1.336(3)
O1–O1′	3.312(2)	3.198(3)

[a] For the numbering see Fig. 2.

Table 3
Calculated bond lengths (Å) of **2**, **12**, **13** and **14** [a]

	2 (C_s)	**12** (C_s)	**13** (C_s)	**14** (D_{5d})
Co–C1	2.103	2.069	2.150	2.060 [b]
Co–C2	2.070	2.059	2.095	
Co–C3	2.073	2.064	2.074	
Co–C4		2.065		
Co–C5		2.061		
Co–C6	2.325	2.129		
Co–C7	2.053	2.064	2.027	
Co–C8	2.004	2.038	1.987	
Co–C9		2.037		
Co–C10		2.063		
C1–C2	1.422	1.424	1.418	1.425 [c]
C1–C5		1.423		
C2–C3	1.433	1.423	1.435	
C3–C4	1.415	1.421	1.414	
C4–C5		1.428		
C6–O1	1.223	1.333		
C6–C7	1.485	1.426		
C6–C10		1.430		
C7–C8	1.418	1.425	1.423	
C8–C9	1.433	1.425	1.422	
C9–C10		1.427		

[a] For the numbering see formulae.
[b] Value for Co–C.
[c] Value for C–C.

five-membered rings of both species. In the case of **4** this comparison shows relatively short distances between the metal and the carbon centers C7–C10, while the distance to C6 is relatively long (2.26(1) Å). Furthermore, the C6–O1 bond is relatively short (1.25(1) Å). In **5** the distances between cobalt and C6–C10 vary only slightly and the C6–O1 distance is longer (1.343(4) Å) than in **4**. This suggests that **4** has a CpCo unit bound to the butadiene fragment of the cyclopentadienone unit while **5** contains an alkoxy substituted cobalticinium system.

Fig. 2 displays the molecular structure of **11** together with the carbon skeleton of the central unit. It shows the same conformation of the propano-chains as in **8** [9]. It is interesting to note that both OH hydrogen atoms are positioned *syn* to each other. The transannular distances increase towards the end with the hydroxy groups. Table 2 contains the most relevant distances of **8** and **11**. Also in this case the same differences are observed as in the case of **4** and **5**. Short distances between the butadiene unit of **8** and the metal and a 'long' distance between cobalt and C6 (2.154(2) Å) as well as a short C6–O1 distance (1.278(2) Å). In **11** the distances between centers C6–C10 and the metal are approximately equal. In **8** the CO groups are more bent apart (O1–O1′ = 3.312(2) Å) than in **11** (O1–O1′ = 3.198(3) Å). This comparison between the structures of **8** and **11** suggests that the CpCo units in **8** interact mainly with the cyclobutadiene system whereas in **11** the two cobalticinium systems are tethered by four propane chains.

3. Theoretical investigations

To check our qualitative interpretation of the bonding in **4**, **5**, **8** and **11** we have carried out density functional theory (DFT) [10] calculations on **2** (R = H), its *O*-protonated species (**12**) as well as on the *cis* butadiene complex $(C_5H_5)Co(C_4H_6)$ (**13**) and cobalticinium $(C_5H_5)_2Co^+$ (**14**) (Formula 2).

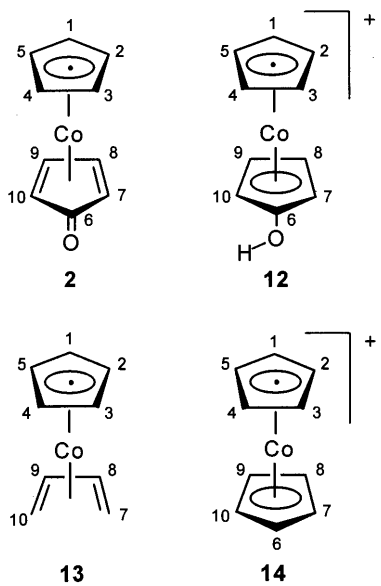

2 **12** **13** **14** (Formula 2)

Table 3 contains the most relevant distances of the optimized structures of **2**, **12**, **13** and **14**. All optimizations were carried out without symmetry constraints. The resulting structures with the exception of **12**, converge to symmetrical species. The structures **2** and **12**–**14** represent minima on the corresponding energy surface.

The optimized structural parameters of the model compounds **2** and **12** agree very well with those of the experimental molecules **4** and **5**. However, the ligands of **4** and **5** adopt an eclipsed conformation, whereas in **2**, **12**, and **14** they are in the staggered position. Since geometry optimization on the eclipsed structure of **14** gave only insignificant increase in energy (2.5 kJ mol^{-1}) we did not further explore the rotation of the ligands in **2** and **12**. Furthermore, as can be expected, the eclipsed **14** has one small imaginary mode (i40 cm^{-1}) which corresponds to the rotation of the cyclopentadienyl ligand. In the complexes **2** and **12**–**14** the average Co–C(Cp) distance does not differ much from those of CpCo (**17**). The free cyclopentadienone ligand **15** adopts a planar structure and the distance of the C7–C8 and C9–C10 double bonds (1.337 Å) is the same as in *cis*-butadiene (**16**) (1.336 Å). Upon complexation with **17**, these bonds are elongated to 1.418 Å (**2**) and 1.423 Å (**13**). In complex **2**, the cyclopentadienone ligand adopts a non-planar structure (torsion angle C6–C7–C8–C9 = 10.2°), and the bond distances C6–C7 and C6–C10 are still long (1.485 Å). In accordance with the X-ray data of **4**, complex **2** displays a long Co–C6 distance (2.325 Å), while the distances between the cobalt atom and the carbon centers C7–C10 are much shorter (2.053, 2.004 Å), and are almost the same as in the *cis*-butadiene complex **13** (2.027, 1.987 Å). The *O*-protonated ligand of complex **12** adopts an almost planar structure (torsion angle C6–C7–C8–C9 = 2.8°), and the bond distances C6–C7 and C6–C10 are shortened to 1.426 and 1.430 Å, respectively. With respect to **2**, the optimized Co–C6 distance of **12** is shorter by 0.196 Å, and does not differ much from the remaining Co–C bonds. The resemblance of the structural parameters of **12** and **14** (Table 3) as well as of **2** and **13** suggests that the particular complexes should have similar electronic structures. To prove this hypothesis, we compare the energy and shapes of the valence MOs of the *cis*-butadiene **16** with those of cyclopentadienone **15** on the left side of Fig. 3. These MOs are derived from the DFT wave functions of the optimized structures. The most striking difference concerns the energy of the LUMO which is by 1.8 eV lower in **15** than in **16**.

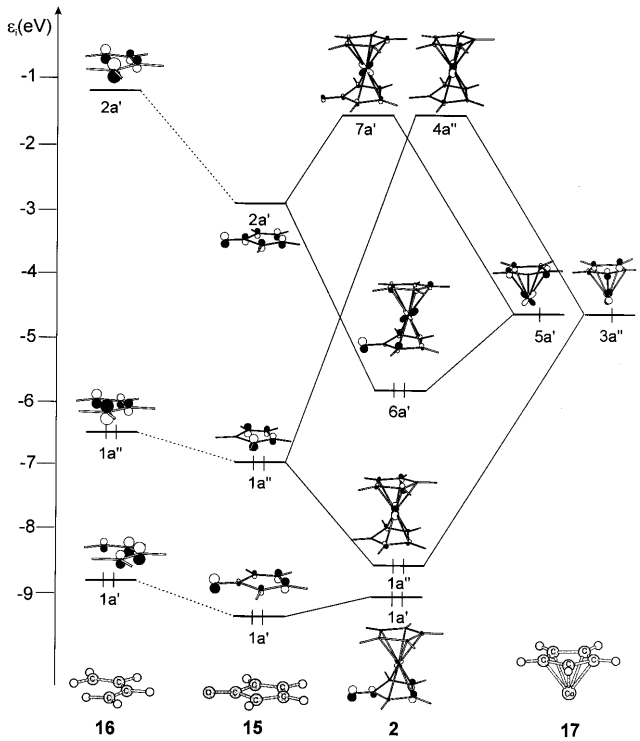

Fig. 3. Interaction diagram between the frontier orbitals of *cis*-butadiene (**16**) and cyclopentadienone (**15**) (left) and two singly occupied MOs of the CpCo fragment (**17**). For the sake of clarity we have omitted at the right side the metal centered Co d_{z^2}, d_{xy} and $d_{x^2-y^2}$ orbitals as well as the orbitals localized at the Cp ring. For the labeling of the MOs we use the irreducible representations of the C_S point group of the resulting complex **2**.

On the right side of Fig. 3 we present a simplified interaction diagram for the complexation of **15** with **17**. The valence MOs of MCp fragments are well known [11], and for the sake of clarity in Fig. 3 only the degenerated HOMO of **17** which has predominantly cobalt character (5a′ (d_{yz}), 3a″ (d_{xz})) is shown. In the region from −9.8 to −5.5 eV we have omitted the doubly occupied 1a′–4a′, and 1a″, 2a″ levels of **17**, which correlate with three cobalt (4a′ ($d_{x^2-y^2}$), 2a″ (d_{xy}), 3a′ (d_{z^2})) and three cyclopentadiene (1a′, 2a′, 1a″) MOs. These MOs do not contribute considerably to the bonding with the ligands. In **2**, the most important bonding interactions are achieved through the mixing of the HOMO (1a″) and LUMO (2a′) of **15** with the degenerated HOMO (5a′, 3a″) of **17**. The resulting 1a″ and 6a′ MOs are strongly stabilized in complex **2**. As a result of the 'Aufbau' principle, the two cobalt electrons from the HOMO of **17** occupy the HOMO (6a′) of **2**, and consequently the interactions in the HOMO (6a′) describe the metal to ligand backbonding. Thus, the 3a″ component of the degenerated HOMO of **17** is virtually empty in complex **2** and can be involved in ligand to metal donating interactions with the 1a″ MO of **15** (Fig. 3). An examination of the charge on the cyclopen-

Table 4
Mulliken net charges q calculated for **2** (R = H), **12**, **13** and **14** [a]

	2	13	12	14
Σ C1–C5	−0.362	−0.447	−0.023	+0.013
C6	+0.330		+0.255	+0.003
Σ C7–C10	−0.586	−0.546	−0.133	+0.010
O1	−0.371	–	−0.064	
Co	+0.989	+0.993	+0.964	+0.974
qL [b]	−0.627	−0.546	+0.058	+0.013

[a] The numbering in **2** corresponds to that used for **4** and **5**. For the numbering of **12**–**14** see formulae.

[b] L = C_4H_4CO (**2**), C_4H_6 (**13**), C_5H_4OH (**12**), C_5H_5 (**14**).

tadienone ligand in complex **2** shows that the metal to ligand backbonding interaction in the HOMO is stronger than the ligand to metal donation interaction in the 1a″ MO (Table 4). From the left side of Fig. 3 it is evident that the stabilizing interactions in complex **13** have the same character as in complex **2**. However, taking into account the high energy of the LUMO of **16**, one can suppose that the backbonding interaction in the HOMO of **13** should be weaker than in **2**. This is in accordance with a smaller negative charge on the *cis*-butadiene ligand in **13** (Table 4) as well as with the calculated binding energies of both ligands. The binding energy of cyclopentadienone in **2** amounts to 392 kJ mol^{-1}, while that of *cis*-butadiene in **13** amounts to 319 kJ mol^{-1}. In summary, the stabilizing interactions in **2** and **13** are of the same character, but due to the low lying LUMO, cyclopentadienone is more stabilized by the metal fragment than *cis*-butadiene.

A comparison between the net charges at the different ligands reveals similarities between **2** and **13** as well as **12** and **14** (Table 4). In **2** and **13** we encounter a strong negative net charge at C1–C5 as well as C7–C10. As a result the negative charge for the hetero ligands L amounts to -0.63 for **2** and -0.55 for **13**. This outcome is anticipated from our discussion of the electronic structure of **2** (Fig. 3). The interaction between the CpCo- and the C_5H_4O-fragment yields to a transfer of electron density from the CpCo fragment to the cyclopentadienone ring in **2**, especially to the butadiene part of the latter.

The comparison between **2** and **12** reveals that protonation changes the charge distribution dramatically. The net charges at both ligands of **12** sum up to $+0.04$. This situation closely resembles that obtained for **14** (Table 4).

4. Experimental

4.1. General remarks

All melting points are uncorrected. The NMR spectra were measured with a Bruker WH 300 (^{1}H-NMR at 300 MHz and ^{13}C-NMR at 75.47 MHz) using the solvent as internal standard (δ). The mass spectra refer to data from a JEOL JMS-700 instrument. IR spectra were recorded with a Bruker Vector 22. UV light absorption data were recorded using a Hewlett Packard 8452A spectrometer. All reactions were carried out in argon atmosphere using dried and oxygen-free solvents.

4.2. Cobalticinium salts *5* and *7*

The amount of 0.1 g of triethyloxonium tetrafluoroborate was added to a 0.35 millimolar solution of the cyclopentadienone complex in 50 ml of dichloromethane. The color changed from orange–red to yellow immediately. The mixture was stirred at room temperature for 48 h. A second portion of 0.09 g of triethyloxonium tetrafluoroborate was added. The solvent was evaporated and the yellow residue purified by column chromatography on alumina (neutral, grade III). With CH_2Cl_2–methanol (20:1) the unreacted complexes (**4** and **6**, respectively) were extracted, followed by the products **5** and **7**, respectively (CH_2Cl_2–methanol (5:1)). For further purification the obtained products were chromatographed again under the same conditions. Yields: 0.05 g (30%) of **5** as green–yellow needles, m.p. 161°C. 0.06 g (30%) of **7** as orange–yellow solid, m.p. 152°C. Further properties of **5**: ^{1}H-NMR ($CDCl_3$): 5.33 (s, 5H, Cp), 4.16–4.10 (q, 2H, CH_2, ethyl), 2.91–2.83 (m, CH_2), 2.74–2.67 (m, CH_2), 2.57–2.44 (m, CH_2), 1.45–1.37 (m, CH_2), 1.35–1.30 (t, 3H, CH_3, ethyl), 1.25–1.01 (m, CH_2). ^{13}C-NMR ($CDCl_3$): 130.3 (s, C–OEt), 96.3 (s, C=C), 89.9 (s, C=C), 85.2 (d, Cp), 70.2 (t, O–CH_2–), 30.7 (t, CH_2), 29.7 (t, CH_2), 25.5 (t, CH_2), 25.4 (t, CH_2), 23.4 (t, CH_2), 23.0 (t, CH_2), 15.5 (q, –CH_3). HRMS (FAB) Anal. Calc. for $[C_{24}H_{34}CoO]^+$: 397.1943. Found: 397.1974. IR (KBr): 2927, 2854, 1633, 1488, 1460, 1350 cm^{-1}. UV–vis (CH_2Cl_2) (λ_{max}, (log ε)): 288 (3.33), 340 (4.81), 398 nm (3.90). Further properties of **7**: ^{1}H-NMR ($CDCl_3$): 5.43 (s, 5H, Cp), 4.35–4.31 (q, 2H, CH_2, ethyl), 3.30–3.22 (m, CH_2), 3.07–3.00 (m, CH_2), 2.88–2.70 (m, CH_2), 2.18–2.16 (m, CH_2), 1.52–1.38 (m, CH_2), 1.47–1.42 (t, 3H, CH_3, ethyl). ^{13}C-NMR ($CDCl_3$): 132.1 (s, C–OEt), 98.4 (s, C=C), 92.1 (s, C=C), 86.3 (d, Cp), 83.9 (s, CC), 82.8 (s, CC), 71.5 (t, O–CH_2), 29.8 (t, CH_2), 27.9 (t, CH_2), 24.1 (t, CH_2), 23.1 (t, CH_2), 19.5 (t, CH_2), 18.9 (t, CH_2), 15.9 (q, CH_3). IR (KBr) 2932, 2863, 1629, 1463, 1461, 1417, 1381 cm^{-1}. UV–vis (CH_2Cl_2) (λ_{max}, (log ε)): 292 nm (4.40). HRMS (FAB) Anal. Calc. for $[C_{28}H_{34}CoO]^+$: 445.1943. Found: 445.1954.

4.3. Ethylation of the cyclopentadienono superphane *8*

A 0.65 g amount of triethyloxonium tetrafluoroborate was added to a solution of 0.2 g (0.35 mmol) of the cyclopentadienono superphane **8** in 100 ml of dichloromethane. The color changed from red–orange to yellow immediately. The mixture was stirred at room temperature for 48 h. A second portion of 0.30 g of triethyloxonium tetrafluoroborate was added after 24 h. The solvent was evaporated and the yellow residue purified by column chromatography on alumina (neutral, grade III). With CH_2Cl_2–methanol (20:1) the monoethylated superphane **9** was extracted first, followed by the twofold ethylated complex **10** (CH_2Cl_2–methanol (10:1)). Finally unreacted **8** was extracted. For further purification the crude products **9** and **10** were chromatographed again under the same conditions. (**9**): Yield 45% (0.10 g), orange solid, m.p. =

Table 5
Crystal data and structure refinement for **4**, **5** and **11**

Compound	**4**	**5**	**11**
Empirical formula	$C_{22}H_{29}CoO$	$C_{24}H_{38}ClCoO_3$	$C_{36}H_{44}Co_2F_6O_{10}$
Formula weight	368.4	468.9	868.6
Crystal color	Yellow	Yellow	Yellow
Crystal shape	Irregular	Irregular	Irregular
Crystal size (mm)	$0.20\times0.25\times0.40$	$0.36\times0.16\times0.10$	$0.28\times0.26\times0.22$
Temperature (K)	293	200	200
Wavelength (Å)	0.71069	0.71073	0.71073
Crystal system	Monoclinic	Monoclinic	Triclinic
Space group	$P2_1/c$	$P2_1/n$	$P\bar{1}$
Z	4	8	2
Unit cell dimensions			
a (Å)	14.124(3)	15.6152(2)	12.3451(2)
b (Å)	10.401(2)	9.9481(2)	12.7423(2)
c (Å)	14.063(3)	30.2950(2)	13.9417(2)
α (°)	90	90	71.103(1)
β (°)	114.96(3)	91.809(1)	87.518(1)
γ (°)	90	90	61.755(1)
V (Å^3)	1873(1)	4703.7(1)	1811.9(1)
D_{calc} (g cm^{-3})	1.31	1.32	1.59
Absorption coefficient, μ (mm^{-1})	0.92	0.87	1.00
θ range for data collection (°)	1.59–20.75	1.34–25.66	1.56–25.62
Index ranges	$-15<h<15$, $-11<k<0$, $0<l<15$	$-18<h<17$, $-12<k<11$, $-35<l<36$	$-14<h<14$, $-14<k<15$, $-16<l<16$
Reflections collected	2177	33 979	13 534
Independent reflections	1935	8142	6040
Max/min transmission	1.00 and 0.88	0.94 and 0.83	0.84 and 0.75
Observed data/parameters	1397/218	8131/577	6040/532
Goodness-of-fit on F^2	2.36	1.07	1.03
$R(F)$	0.062	0.045	0.037
$R_w(F^2)$	0.197	0.084	0.096
$(\Delta\rho)$max, $(\Delta\rho)$min (e Å^{-3})	0.54, −0.60	0.58, −0.48	0.73, −0.57

182°C. ^{1}H-NMR ($CDCl_3$): 5.22 (s, 5H, Cp), 4.53 (s, 5H, Cp), 4.15–4.11 (q, 2H, CH_2, ethyl), 2.98–2.55 (m, CH_2), 2.27–2.14 (m, CH_2), 1.86–1.83 (m, CH_2), 1.41–1.38 (t, 3H, CH_3, ethyl). ^{13}C-NMR ($CDCl_3$): 127.2 (s, C–OEt), 93.4 (s, C=C), 92.7 (s, C=C), 90.4 (s, C=C), 84.7 (d, Cp), 82.6 (s, C=C), 82.5 (d, Cp), 68.8 (t, O–CH_2–), 25.3 (t, CH_2), 23.7 (t, CH_2), 23.4 (t, CH_2), 23.1 (t, CH_2), 23.0 (t, CH_2), 21.9 (t, CH_2), 15.4 (q, –CH_3). HRMS (FAB) Anal. Calc. for $[C_{34}H_{39}Co_2O_2]^+$: 597.1616. Found: 597.1639. IR (KBr) 2925, 1632, 1527, 1455, 1415 cm^{-1}. UV–vis (CH_2Cl_2) (λ_{max}, (log ε)): 286 (4.24), 316 (4.66), 366 nm (4.08). (**10**) 11% (27 mg) green–yellow needles, m.p. >250°C. ^{1}H-NMR ($CDCl_3$, CD_3OD): 5.41 (s, 5H, Cp), 4.32–4.25 (q, 2H, CH_2, ethyl), 3.02–2.73 (m, CH_2), 2.52–2.02 (m, CH_2), 1.61–1.56 (t, 3H, CH_3, ethyl). ^{13}C-NMR ($CDCl_3$): 128.5 (s, C–OEt), 94.2 (s, C=C), 93.2 (s, C=C), 85.6 (d, Cp), 71.6 (t, O–CH_2–), 25.3 (t, CH_2), 23.8 (t, CH_2), 23.0 (t, CH_2), 22.5 (t, CH_2), 15.4 (q, –CH_3). HRMS (FAB) Anal. Calc. for $[C_{36}H_{44}Co_2O_2]^+$: 626.2007. Found: 626.2045. IR (KBr) 3098, 2929, 1630, 1487, 1464, 1383, 1355 cm^{-1}. UV–vis (CH_2Cl_2) [λ_{max}, (log ε)]: 326 nm (4.97).

4.4. Twofold protonation of the cyclopentadienono superphane **8**

The cyclopentadienono superphane **8** was dissolved in a mixture of chloroform (5 ml) and methanol (5 ml). To this solution 5 ml of trifluoroacetic acid was added. The color changed from red–orange to green–yellow immediately. After the solvents had been evaporated at room temperature green–yellow needles of **11** were isolated. Yield >95% (67 mg) m.p. >250°C. ^{1}H-NMR ($CDCl_3$, CD_3OD, CF_3COOD, 5:5:1): 4.92 (s, 5H, Cp), 2.88–2.33 (m, 2H, CH_2), 2.65–2.60 (m, CH_2), 2.55–2.41 (m, CH_2), 2.23–2.12 (m, CH_2), 1.95–1.91 (m, CH_2). ^{13}C-NMR ($CDCl_3$): 128.0 (s, C–OD), 93.0 (s, C=C), 91.4 (s, C=C), 85.7 (d, Cp), 25.4 (t, CH_2), 23.4 (t, CH_2), 22.4 (t, CH_2) HRMS (FAB) Anal. Calc. for $[C_{32}H_{35}Co_2O_2]^+$ ($M^{2+}-H^+$): 569.1303. Found:

569.1337. IR (KBr): 2941, 1732, 1510, 1474, 1450 cm^{-1}. UV–vis (CH_2Cl_2) (λ_{max}, (log ε)): 324 nm (4.53).

4.5. Calculation details

A single all-electron basis set has been employed in this work. For Co we have chosen Wachters' (14s, 9p, 5d) basis set [12] augmented with a 4f polarization function ($\alpha_f = 1.117$). The contraction scheme corresponds to a double- and triple-ξ basis for the core and valence electrons, respectively. The 6-311G basis set [13] was used for C, O, and H. The basis set of C and O was augmented by a single 3d polarization function ($\alpha_C = 0.626$, $\alpha_O = 1.292$). The geometries of the investigated compounds were fully optimized, and harmonic vibration frequencies were calculated at the DFT level by using the three-parameter fit of the functional, known in the literature as the B3LYP method [14].

The calculations were carried out with the GAUSSIAN-98 program [15]. For graphical displays we used the MOLEK-9000 [16] and GAUSSVIEW [17] programs.

4.6. X-ray crystallography and structure solution

The crystallographic data were recorded with a Syntex R3 (**4** at 293 K) and a Siemens Smart CCD diffractometer (**5**, **11** at 200 K). Relevant crystal and data collection parameters are given in Table 5. The structures were solved by using direct methods, least-squares refinement, and Fourier techniques. Structure solution and refinement were performed with SHELXTL [18].

5. Supplementary material

Crystallographic data (excluding structure factors) for the structural analysis has been deposited with the Cambridge Crystallographic Data Centre, CCDC nos. 143541 (**4**), 143542 (**5**) and 143543 (**11**). Copies of this information may be obtained free of charge from: The Director, CCDC, 12 Union Road, Cambridge, CB2 1EZ, UK (fax: +44-1223-336033; e-mail: deposit@ccdc.cam.ac.uk or www: http://www.ccdc.cam.ac.uk).

Acknowledgements

We are grateful to the Deutsche Forschungsgemeinschaft (SFB 247), the Fonds der Chemischen Industrie and the BASF Aktiengesellschaft, Ludwigshafen, for financial support.

References

[1] Review: M.A. Ogliaruso, M.G. Romanelli, E.I. Becker, Chem. Rev. 65 (1965) 261 and references therein.
[2] (a) K. Hafner, K. Goliasch, Chem. Ber. 94 (1961) 2909. (b) C.H. DePuy, M. Isaks, K.L. Eilers, G.F. Morris, J. Org. Chem. 29 (1964) 3503.
[3] E.W. Garbisch, R.F. Sprecher, J. Am. Chem. Soc. 91 (1968) 6785 and references therein.
[4] Reviews: (a) W. Hübel, in: I. Wender, P. Pino (Eds.), Organic Synthesis via Metal Carbonyls, vol. 1, Wiley, New York, 1968, p. 273. (b) P. Pino, G. Braca, in: I. Wender, P. Pino (Eds.), Organic Synthesis via Metal Carbonyls, vol. 2, Wiley, New York, 1977, p. 419. (c) N.E. Schore, Chem. Rev. 88 (1988) 1081.
[5] G.N. Schrauzer, G. Kratel, J. Organomet. Chem. 2 (1964) 336.
[6] P. Jutzi, U. Siemeling, A. Müller, H. Bögge, Organometallics 8 (1989) 1744.
[7] (a) J.E. Sheats, M.D. Rausch, J. Org. Chem. 35 (1970) 3245. (b) R.E. Benson, R.V. Lindsey, J. Am. Chem. Soc. 79 (1957), 5471. (c) R. Markby, H.W. Sternberg, I. Wender, Chem. Ind. (London) (1959) 1381.
[8] R. Boese, D. Bläser, R.L. Halterman, K.P.C. Vollhardt, Angew. Chem. 100 (1988) 592; Angew. Chem., Int. Ed. Engl. 27 (1988) 553.
[9] (a) R. Roers, F. Rominger, C. Braunweiler, R. Gleiter, Tetrahedron Lett. 39 (1998) 7831. (b) R. Roers, F. Rominger, B. Nuber, R. Gleiter, Organometallics 19 (2000) 1578.
[10] (a) W. Kohn, L.J. Sham, Phys. Rev. A 140 (1965) 1133. (b) R.G. Parr, W. Yang, Density Functional Theory of Atoms and Molecules, Oxford University Press, Oxford, 1969.
[11] T.A. Albright, J.K. Burdett, M.-H. Whangbo, Orbital Interactions in Chemistry, Wiley, New York, 1995.
[12] A.J.H. Wachters, J. Chem. Phys. 52 (1970) 1033.
[13] R. Krishnan, J.S. Binkley, R. Seeger, J.A. Pople, J. Chem. Phys. 72 (1980) 650.
[14] (a) A.D. Becke, J. Chem. Phys. 96 (1992) 2155. (b) A.D. Becke, J. Chem. Phys. 98 (1993) 5648. (c) S.H. Vosko, L. Wilk, M. Nusair, Can. J. Phys. 58 (1980) 1200. (d) C. Lee, W. Yang, R.G. Parr, Phys. Rev. B. 37 (1988) 785.
[15] We used GAUSSIAN-98 (Rev. A5) program by M.J. Frisch, G.W. Trucks, H.B. Schlegel, G.E. Scuseria, M.A. Robb, J.R. Cheeseman, V.G. Zakrzewski, J.A. Montgomery Jr., R.E. Stratmann, J.C. Burant, S. Dapprich, J.M. Millam, A.D. Daniels, K.N. Kudin, M.C. Strain, O. Farkas, J. Tomasi, V. Barone, M. Cossi, R. Cammi, B. Mennucci, C. Pomelli, C. Adamo, S. Clifford, J. Ochterski, G.A. Petersson, P.Y. Ayala, Q. Cui, K. Raghavachari, J.B. Foresman, J. Cioslowski, J.V. Ortiz, B.B. Stefanov, G. Liu, A Liashenka, P. Piskorz, I. Komaromi, R. Gomoerts, R.L. Martin, D.J. Fox, T. Keith, M.A. Al-Laham, C.Y. Peng, A. Nanyakkara, C. Gonzalez, M. Challacombe, P.M.W. Gill, B. Johnson, W. Chen. M.W. Wong, J.L. Andres, C. Gonzalez, M. Head-Gordon, E.S. Replogle, J.A. Pople, Gaussian Inc., Pittsburgh, PA, 1998.
[16] P. Bischof, MOLEK-9000, Universität Heidelberg.
[17] GAUSSVIEW, Gaussian Inc., Pittsburgh, PA, 1998.
[18] G.M. Sheldrick, Bruker Analytical X-ray Division, Madison, WI, 1997.